Institute of Paper Science and Technology
Atlanta, Georgia

IPST Technical Paper Series Number 773

Exact and Approximate Expressions for Bubble/Particle Collision

T. Heindel and F. Bloom

March 1999

Submitted to
Journal of Colloid and Interface Science

INSTITUTE OF PAPER SCIENCE AND TECHNOLOGY
PURPOSE AND MISSIONS

The Institute of Paper Science and Technology is an independent graduate school, research organization, and information center for science and technology mainly concerned with manufacture and uses of pulp, paper, paperboard, and other forest products and byproducts. Established in 1929, the Institute provides research and information services to the wood, fiber, and allied industries in a unique partnership between education and business. The Institute is supported by 52 North American companies. The purpose of the Institute is fulfilled through four missions, which are:

- to provide a multidisciplinary education to students who advance the science and technology of the industry and who rise into leadership positions within the industry;
- to conduct and foster research that creates knowledge to satisfy the technological needs of the industry;
- to serve as a key global resource for the acquisition, assessment, and dissemination of industry information, providing critically important information to decision-makers at all levels of the industry; and
- to aggressively seek out technological opportunities and facilitate the transfer and implementation of those technologies in collaboration with industry partners.

ACCREDITATION

The Institute of Paper Science and Technology is accredited by the Commission on Colleges of the Southern Association of Colleges and Schools to award the Master of Science and Doctor of Philosophy degrees.

NOTICE AND DISCLAIMER

The Institute of Paper Science and Technology (IPST) has provided a high standard of professional service and has put forth its best efforts within the time and funds available for this project. The information and conclusions are advisory and are intended only for internal use by any company who may receive this report. Each company must decide for itself the best approach to solving any problems it may have and how, or whether, this reported information should be considered in its approach.

IPST does not recommend particular products, procedures, materials, or service. These are included only in the interest of completeness within a laboratory context and budgetary constraint. Actual products, procedures, materials, and services used may differ and are peculiar to the operations of each company.

In no event shall IPST or its employees and agents have any obligation or liability for damages including, but not limited to, consequential damages arising out of or in connection with any company's use of or inability to use the reported information. IPST provides no warranty or guaranty of results.

Exact and Approximate Expressions for Bubble/Particle Collision

Theodore J. Heindel[†] and Frederick Bloom[*]

[†] Engineering Division, Institute of Paper Science and Technology, 500 10th St., N.W., Atlanta, GA 30318

[*] Department of Mathematical Sciences, Northern Illinois University, DeKalb, IL 60115

Suggested Running Title: Bubble/Particle Collision

Corresponding Author: Theodore J. Heindel
Institute of Paper Science and Technology
500 10th Street, NW
Atlanta, GA 30318-5794
Ph: 404-894-8264
Fax: 404-894-4778
E-mail: ted.heindel@ipst.edu

Abstract

The flotation microprocess of collision is investigated and an exact expression for the probability of collision (P_c) is developed based on the intermediate flow of Yoon and Luttrell (1). This expression for P_c only assumes that the bubble and particle are spherical and that the particle radius is less than the bubble radius (i.e., $R_p < R_B$). In addition to removing the requirement that $R_p << R_B$, the influence of a particle settling velocity is also included in the model development. The expression for P_c is shown to be a function of three dimensionless groups: (i) the magnitude of the dimensionless particle settling velocity, $|G|$; (ii) the bubble Reynolds number, Re_B; and (iii) the ratio of particle to bubble radius, R_p/R_B.

The probability of collision model is compared to available experimental data and good agreement is shown. A parametric study is also completed for $0 \leq |G| \leq 1$, $0 \leq Re_B \leq 500$, and $0.001 \leq R_p/R_B < 1$. In general, P_c is independent of Re_B when $R_p/R_B \lesssim 0.03$, the particle settling velocity is important for small values of R_p/R_B, and R_p/R_B dominates as $R_p/R_B \rightarrow 1$.

Key Words: capture; collision; flotation; microprocess probability; particle settling velocity

Introduction

Flotation separation is used in many industries such as mineral processing, petrochemical refining, water treatment, and pulp and paper manufacturing. In the paper industry, flotation is used in paper recycling to separate inks and other contaminants from useable cellulose fiber. This separation process is called flotation deinking, and is accomplished by injecting air bubbles into an agitated liquid tank containing suspended cellulose fibers and contaminant particles (including inks and toners). The air bubbles preferentially attach to hydrophobized contaminant particles and transport them to the froth layer where they may be easily removed.

The basic viewpoint that has been taken in modeling the overall flotation separation process is that it is a multi-stage probability process consisting of a sequence of microprocesses with associated probability measures. This sequence includes the approach of a particle to an air bubble, the subsequent interception of that particle by the bubble, the sliding of the particle along the surface of the thin liquid film that separates the particle from the bubble, film rupture, the subsequent formation of a three-phase contact between the bubble, particle, and liquid, and the stabilization of the bubble/particle aggregate (with its subsequent transport to the froth layer for removal from the flotation cell).

Probability measures, which are associated with some of the elementary microprocesses have appeared in many places in the literature. In this paper we develop new, exact, expressions for P_c, the microprocess probability of collision (or capture) of a particle by a bubble. In the analysis to follow, all particles and all bubbles in any given volume of the flotation cell are assumed to be perfectly spherical.

As indicated in Fig. 1, only those particles which approach a rising bubble within a streaming tube of limiting capture radius R_c can collide with or be intercepted by a bubble.

Once an expression has been determined for R_c, the probability P_c is then computed to be the ratio of the number of particles with $R_p < R_B$ which encounter a bubble per unit time to the number of particles which approach a bubble in a stream tube with cross section equal to $\pi(R_p + R_B)^2$; this ratio is easily determined to be given by

$$P_c = \left(R_c/(R_p + R_B)\right)^2 \qquad [1]$$

where R_p and R_B are the particle and bubble radius, respectively.

Many authors simply take $P_c = \left(R_c/R_B\right)^2$, e.g. Yoon and Luttrell (1); however, as these authors note, "the denominator should actually be $R_B + R_p$ but (the) equation holds when $R_B >> R_p$". Because one of our goals is the derivation of exact expressions for P_c, we choose not to make any approximations which are based upon assumptions concerning the relative magnitudes of R_p and R_B until the final stages of the analysis.

The determination of an expression for R_c in [1] is a nontrivial exercise which has occupied the attention of many researchers in collodial hydrodynamics during the past six decades since the original work of Sutherland (2) (which dealt with potential flow around the bubble in the absence of both inertial forces and gravitational effects); principal contributions in this area include the work of Yoon and Luttrell (1, 3), Ahmed and Jameson (4), Schulze (5, 6), Flint and Howarth (7), Nguyen-Van and Kmet (8), Nguyen-Van (9), Weber (10), Weber and Paddock (11), Reay and Ratcliff (12), Dobby and Finch (13), Anfruns and Kitchener (14, 15), Spielman (16), and Michael and Norey (17). During the course of this analysis, we will have occasion to refer to specific results in several of the papers referenced above and, in particular, will indicate the manner in which many of those results are either special cases of or approximations to the more exact relations that are derived below.

The specific derivation of expressions for the capture radius R_c is dependent upon the

basic assumptions one makes about the relationship between R_p and R_B, the nature of the flow field in which the particle moves, and the role (or lack thereof) of inertial and gravitational forces in the process. At this stage of the overall flotation process, i.e., the approach of a particle to a bubble, only the long-range hydrodynamic interaction is taken into account as opposed to those short-range hydrodynamic interactions which must be considered once the particle has intercepted the bubble and begins the sliding process over the thin film which separates the particle from the bubble. A rather comprehensive discussion of the overall flotation deinking process may be found in (18-20).

Among the key parameters which arise in any discussion of the flow field in the neighborhood of a rising bubble are the bubble Reynolds number

$$Re_B = \frac{v_B d_B \rho_\ell}{\mu_\ell} \qquad [2]$$

and the Stokes number

$$St = \frac{\rho_p d_p^2 v_B}{9\mu_\ell d_B} = \frac{Re_B \rho_p d_p^2}{9\rho_\ell d_B^2} \qquad [3]$$

which is the ratio of the inertial force of the particle to the viscous drag force of the bubble. In the above equations, v_B is the bubble rise velocity, d_B and d_p are the bubble and particle diameter, ρ_p and ρ_ℓ are the particle and liquid density, and μ_ℓ is the liquid dynamic viscosity. Much of the earlier literature on flotation processes was concerned with mineral flotation for which $0.1 < St < 1$ is a reasonable assumption; however, some of the later work in that area, as well as almost all the work on flotation deinking, has been concerned with the situation in which $St << 0.1$ so that inertial forces, in essence, no longer influence particle motion. Under these circumstances, it is still possible for particle paths to deviate slightly from the streamlines of the flow if one accounts for particle settling velocity.

In the present work three types of flow will be discussed: potential flow, Stokes flow, and

the intermediate flow of Yoon and Luttrell (1, 3); our main interest is in the latter class of flows as previously discussed in (18); the class of intermediate flows introduced in (1) has also been incorporated into the work of Schulze (5) and Nguyen-Van (9) and discussed in the recent survey paper of Matis and Zouboulis (21). For all three of the flows listed above we shall assume that the flow streamlines are symmetrical, fore and aft, with respect to the bubble surface; such an assumption was explicitly employed by Yoon and Luttrell (1) and implies that a grazing trajectory may be defined as the one which, at the bubble equator, passes within a distance of particle radius R_p from the bubble surface (Fig. 1). Clearly, such a trajectory, when traced back an infinite distance from the bubble surface, passes precisely within a distance R_c of the stagnation line of the flow which passes through the bubble center. Fore and aft asymmetry has been discussed by Clift et al. (22), and if one does not assume that the grazing trajectory occurs at $\theta = \frac{\pi}{2}$ in Fig. 1, then a collision angle θ_c must be introduced, θ_c being the angle on the bubble surface, measured from the front stagnation point, over which particle interception by the surface is possible. The recent work of Nguyen-Van (9) indicates that $\theta_c = \pi/2$ for the intermediate flow of Yoon and Luttrell (1), as well as for potential flow and creeping Stokes flow, is a reasonable assumption. Cases for which $\theta_c \neq \pi/2$ have been discussed in (8-13).

In order to determine the trajectory of a particle approaching a rising bubble, one begins by considering, in Cartesian coordinates, the forces which act on a typical particle. In this paper we let $\mathbf{v}_p$ represent the particle velocity, and v_{px} and v_{py}, the x and y components, respectively, of the particle velocity field.

Accounting for the drag, buoyancy, and gravitational forces, a system of equations rep-

resenting the particle motion may be written as

$$\begin{cases} \frac{4}{3}\pi\rho_p R_p^3 \frac{dv_{px}}{dt} &= -f(v_{px} - u_x) \\ \frac{4}{3}\pi\rho_p R_p^3 \frac{dv_{py}}{dt} &= \frac{4}{3}\pi R_p \Delta\rho g - f(v_{py} - u_y) \end{cases} \qquad [4]$$

where f is the friction factor and $\Delta\rho = \rho_p - \rho_\ell$. For Stokesian particles it is well know that $f = 6\pi\mu_\ell R_p$ in which case the drag force is given by $\mathbf{F}_d = 6\pi\mu_\ell R_p \mathbf{v}_p$. For non-Stokesian particles we have, in general, $\mathbf{F}_d = f\mathbf{v}_p$ while the coefficient of drag, C_D, is defined to be

$$C_D = \frac{f}{\frac{1}{2}\rho_\ell |\mathbf{v}_p| \pi R_p^2} \qquad [5]$$

In the Stokesian case, with $f = 6\pi\mu_\ell R_p$ and $C_D = C_D^{st}$, [5] yields

$$C_D^{st} = 12\nu_\ell / R_p |\mathbf{v}_p| \qquad [6]$$

where ν_ℓ is the liquid kinematic viscosity ($\nu_\ell = \mu_\ell/\rho_\ell$). If we define, in the usual manner, the Reynolds number for the particle to be

$$Re_p = \frac{2R_p|\mathbf{v}_p|}{\nu_\ell} \qquad [7]$$

then [6] and [7] yield the widely known result (e.g., Cheremisinoff (23)) that $C_D^{st} = 24/Re_p$. In the general case, however, it is easily seen that [5] and [7] combine so as to yield

$$C_D = \frac{4f}{(\pi\mu_\ell R_p) Re_p} \qquad [8]$$

It is generally accepted (23) that $C_D = C_D^{st} = 24/Re_p$ holds for $Re_p < 2$. For the situation that is considered below, in which inertial forces acting on the particle are ignored (so that, in effect, the Stokes number $St = 0$), the particle velocity corresponds to the particle settling velocity ($\mathbf{v}_p = \mathbf{v}_{ps}$). In this case it can be demonstrated (23) that

$$C_D Re_p^2 = \frac{4}{3} Ar \qquad [9]$$

where the Archimedes number Ar is the dimensionless parameter defined by

$$Ar = \frac{\Delta\rho}{\rho_\ell}\frac{d_p^3 g}{\nu_\ell^2} \qquad [10]$$

For the Stokes' law range ($Re_p < 2$), the use of $C_D = C_D^{st} = \frac{24}{Re_p}$ in [9] leads to $Re_p = \frac{Ar}{18}$. In the intermediate or transitional range in which $2 < Re_p < 500$ empirical results must be used; from the results reported in (23) we infer that

$$C_D = \frac{18.5}{Re_p^{0.6}}, \quad 2 < Re_p < 500 \qquad [11]$$

the use of which in [9] yields

$$Re_p = 0.152 Ar^{0.715}, \quad 2 < Re_p < 500 \qquad [12]$$

By combining [8] with [9] we find that, in general

$$f = \frac{\pi\mu_\ell R_p}{3}\frac{Ar}{Re_p} \qquad [13]$$

From [13], with $Re_p = \frac{Ar}{18}$ for Stokesian particles, we recover the usual friction factor $f = 6\pi\mu_\ell R_p$ associated with the Stokes flow regime, while for $2 < Re_p < 500$ the required result for f is obtained by combining [13] with the empirical relation [12].

For the analysis which follows, it is convenient to introduce the dimensionless factor

$$\lambda \equiv 6\pi\mu_\ell R_p / f = 18 Re_p / Ar \qquad [14]$$

by virtue of [13]. Clearly $\lambda = 1$ for Stokesian particles ($Re_p < 2$) while in the transitional domain ($2 < Re_p < 500$) λ may be computed by combining [14] with the empirical relation [12].

Instead of working with the system [4] we may nondimensionalize the equations by introducing the variables

$$\mathbf{v}_p^* = \frac{\mathbf{v}_p}{v_B}, \quad \mathbf{u}^* = \frac{\mathbf{u}}{v_B}, \quad t^* = \frac{tv_B}{R_B} \tag{15}$$

A straightforward calculation, and using the dimensionless factor λ, yields the system

$$\begin{cases} \lambda St \dfrac{dv_{px}^*}{dt^*} = -(v_{px}^* - u_x^*) \\ \lambda St \dfrac{dv_{py}^*}{dt^*} = \dfrac{2R_p^2 \triangle \rho g}{9\mu_\ell v_B}\lambda - (v_{py}^* - u_y^*) \end{cases} \tag{16}$$

We now set

$$\tilde{v}_{ps} = -\frac{2R_p^2 \triangle \rho g}{9\mu_\ell} \tag{17}$$

and

$$G = \lambda \frac{\tilde{v}_{ps}}{v_B} \equiv \frac{v_{ps}}{v_B} \tag{18}$$

According to our sign convention $v_B > 0$ so that $v_{ps} < 0$; thus, we also have $G < 0$. In [17] and [18], $\tilde{v}_{ps}$ represents the (terminal) particle settling velocity for Stokesian particles, $v_{ps} = \lambda \tilde{v}_{ps}$ is the true particle settling velocity, and G is the dimensionless particle settling velocity. For Stokesian particles, therefore, $G = \tilde{v}_{ps}/v_B$.

Using the definitions [17] and [18], in [16], assuming that $St \simeq 0$, so that inertial effects are discounted, and noting that $-v_{ps} = |v_{ps}|, -G = |G|$, we easily find that

$$\begin{cases} v_{px}^* = u_x^* \\ v_{py}^* = |G| + u_y^* \end{cases} \tag{19}$$

The system [19] has appeared in Flint and Howarth (7) and Schulze (6); however, in these references it has been assumed that $G \equiv \tilde{v}_{ps}/v_B$, which is only valid for Stokes flow.

Exact and Approximate Expressions for P_c

We begin the analysis by recalling that in [1] R_c represents the largest distance from the stagnation line through the center of the rising bubble, within which a particle path trajectory can pass so that the particle surface will graze the bubble surface at $\theta = \pi/2$, i.e., the maximal distance so that $r = R_B + R_p$ along the particle path trajectory when $\theta = \pi/2$. By virtue of [19], particle path trajectories are coincident with fluid streamlines when $G = 0$. Also, from Fig. 1, it is clear that there exists a smallest r, say, $r = r_c$ with the property that, along a particle path trajectory, an approaching particle will be at the distance R_c from the stagnation line through the center of a rising bubble for all $r \geq r_c$. We now define θ_0 by

$$\sin\theta_0 = R_c/r_c \qquad [20]$$

and note that

$$\sin\theta = \frac{R_c}{r}, \quad \text{for all } r \geq r_c \qquad [21]$$

Our first task is the derivation of an exact expression for P_c for the case of the intermediate flow delineated in Yoon and Luttrell (1). The stream function for 'intermediate flow' (as given in (1)), has the form

$$\psi^{int} = v_B R_B^2 \sin^2\theta \left[\frac{1}{2}r^{*^2} - \frac{3}{4}r^* + \frac{1}{4r^*} + Re_B^* \left(\frac{1}{r^{*2}} - \frac{1}{r^*} + r^* - 1\right)\right] \qquad [22]$$

where

$$Re_B^* = \frac{1}{15}Re_B^{0.72}, \quad r^* = r/R_B \qquad [23]$$

It is noted that the widely-used stream function empirically determined by Yoon and Luttrell (1) predicts a zero radial liquid velocity at $\theta = \pi/2$; however, experiments by Seeley et al. (24) show that this velocity is nonzero.

We now rewrite the system of equations [19] in 'polar coordinates' (actually, spherical coordinates projected onto the x, y plane) as

$$\begin{cases} v^*_{p\theta} = |G| \sin\theta + u^*_\theta \\ v^*_{pr} = -|G| \cos\theta + u^*_r \end{cases} \qquad [24]$$

where

$$u^*_\theta = u_\theta / v_B, \quad u^*_r = u_r / v_B \qquad [25]$$

and the subscripts θ and r represent the angular and radial velocity components of the respective velocities.

The system [24] is identical to the similar (dimensionless) system in Flint and Howarth (7) except for the interpretation of G that has already been noted. The dimensional form of [24] is

$$\begin{cases} v_{p\theta} = u_\theta + v_B |G| \sin\theta \\ v_{pr} = u_r - v_B |G| \cos\theta \end{cases} \qquad [26]$$

so that the radial and tangential components of the particle velocity field $\mathbf{v}_p$ are computable once the radial and tangential components of the fluid velocity field have been specified; in [26], $v_B G = v_{ps} \equiv \lambda \tilde{v}_{ps}$, the (dimensional) particle settling velocity.

If Ψ^* is the dimensionless particle trajectory stream function (see, e.g., Batchelor (25), §2.2) then

$$\begin{cases} v^*_{p\theta} = \dfrac{1}{r^* \sin\theta} \dfrac{\partial \Psi^*}{\partial r^*} \\ v^*_{pr} = -\dfrac{1}{r^{*2} \sin\theta} \dfrac{\partial \Psi^*}{\partial \theta} \end{cases} \qquad [27]$$

and the dimensional form of the particle trajectory stream function is obtained from

$$\Psi = v_B R_B^2 \Psi^* \qquad [28]$$

If $\mathbf{u}^{int}$ is the fluid velocity field which corresponds to the intermediate flow of Yoon and Luttrell (1) then

$$\begin{cases} v_B R_B^2 \dfrac{1}{r\sin\theta}\dfrac{\partial \Psi^{*int}}{\partial r} = u_\theta^{int} + v_B|G|\sin\theta \\ -v_B R_B^2 \dfrac{1}{r^2\sin\theta}\dfrac{\partial \Psi^{*int}}{\partial \theta} = u_r^{int} - v_B|G|\cos\theta \end{cases} \qquad [29]$$

However,

$$\begin{cases} u_\theta^{int} = v_B R_B^2 \dfrac{1}{r\sin\theta}\dfrac{\partial \psi^{*int}}{\partial r} \\ u_r^{int} = -v_B R_B^2 \dfrac{1}{r^2\sin\theta}\dfrac{\partial \psi^{*int}}{\partial \theta} \end{cases} \qquad [30]$$

where ψ^{*int} is the dimensionless form of [22].

By combining [29] and [30] we easily obtain the system

$$\begin{cases} \dfrac{\partial \Psi^{*int}}{\partial r} = \dfrac{\partial \psi^{*int}}{\partial r} + \dfrac{|G|}{R_B^2} r\sin\theta \\ \dfrac{\partial \Psi^{*int}}{\partial \theta} = \dfrac{\partial \psi^{*int}}{\partial \theta} + \dfrac{1}{2}\dfrac{|G|}{R_B^2} r^2 \sin 2\theta \end{cases} \qquad [31]$$

Partially integrating these two equations and solving for the unknow constants yields

$$\Psi^{*int} = \psi^{*int} + \frac{1}{2}\frac{|G|}{R_B^2} r^2 \sin^2\theta \qquad [32]$$

Using the appropriate expression for Ψ^{*int} and rearranging, we obtain for the dimensional particle trajectory stream function associated with the intermediate flow of Yoon and Luttrell (1)

$$\Psi^{int} = v_B R_B^2 \sin^2\theta \left\{ \left[\frac{1}{2}(1+|G|)\frac{r^2}{R_B^2} - \frac{3}{4}\frac{r}{R_B} + \frac{1}{4}\frac{R_B}{r} \right] + Re_B^* \left[\frac{R_B^2}{r^2} - \frac{R_B}{r} + \frac{r}{R_B} - 1 \right] \right\} \qquad [33]$$

We observe that [33] reduces to the result cited in Flint and Howarth (7), for the case of Stokes' flow, with $St = 0$, $G \neq 0$, when $Re_B^* = 0$; however, $Re_B^* = 0 \Leftrightarrow Re_B = 0$ is precisely the condition under which the intermediate flow of Yoon and Luttrell (1) reduces to Stokes flow around the bubble.

We now employ Ψ^{int}, as given by [33], to compute P_c for an intermediate flow around the bubble when $St = 0$ and $G \neq 0$. The grazing trajectory generated by the particle path stream function in [33] satisfies

$$\Psi^{int}(r,\theta) = \text{const.} \equiv \Psi^{int}\left(R_p + R_B, \frac{\pi}{2}\right) \qquad [34]$$

Employing [34] in [33], assuming that $r \geq r_c$, so that $\sin\theta = R_c/r$, and then letting $r \to \infty$, we find that

$$\begin{aligned} R_c^2 = \frac{1}{1+|G|}\Bigg\{&\left[(R_p+R_B)^2(1+|G|) - \frac{3}{2}R_B(R_p+R_B) + \frac{1}{2}\frac{R_B^3}{R_p+R_B}\right] \\ &+2Re_B^*\left[\frac{R_B^4}{(R_p+R_B)^2} - \frac{R_B^3}{R_p+R_B} + R_B(R_p+R_B) - R_B^2\right]\Bigg\} \end{aligned} \qquad [35]$$

Therefore, after some simplification, as an exact expression for P_c in this case we obtain (recall that $P_c = R_c^2/(R_B+R_p)^2$):

$$\boxed{\begin{aligned} P_c^{int} = \frac{1}{1+|G|}\Bigg[&\frac{1}{2(R_p+R_B)^3}\{2R_p^3 + 3R_p^2R_B\} \\ &+\frac{2Re_B^*}{(R_p+R_B)^4}\{R_BR_p^3 + 2R_B^2R_p^2\}\Bigg] + \frac{|G|}{1+|G|} \end{aligned}} \qquad [36]$$

For intermediate flow, in the sense of Yoon and Luttrell (1), with the particle settling velocity assumed to be negligible, we may set $G = 0$ in [36] so as to obtain

$$\begin{aligned} \hat{P}_c^{int} = &\frac{1}{2(R_p+R_B)^3}\{2R_p^3 + 3R_p^2R_B\} \\ &+\frac{2Re_B^*}{(R_p+R_B)^4}\{R_BR_p^3 + 2R_B^2R_p^2\} \end{aligned} \qquad [37]$$

On the other hand, setting $Re_B^* = 0 \Leftrightarrow Re_B = 0$ in [36] yields the exact collision probability for Stokes' flow around the bubble with $St = 0, G \neq 0$, i.e.

$$P_c^{st} = \frac{1}{1+|G|}\left[\frac{1}{2(R_p+R_B)^3}\{2R_p^3 + 3R_p^2R_B\}\right] + \frac{|G|}{1+|G|} \qquad [38]$$

Finally, for Stokes' flow around the bubble with $St = 0$ and $G = 0$, [38] yields

$$\hat{P}_c^{st} = \frac{1}{2(R_p + R_B)^3}\{2R_p^3 + 3R_p^2 R_B\} \qquad [39]$$

The expressions [36] and [37] for intermediate flow and [38] and [39] for Stokes flow around the bubble are *exact relations* which depend only on the hypotheses that $St \approx 0$ and that the fluid flow streamlines are symmetric fore and aft of the bubble so that the collision angle $\theta_c = \pi/2$ (in both [37] and [39] we also assume that $G \approx 0$). To the best of the authors' knowledge, the *exact* expressions in [36]-[39] have not appeared previously in the literature. What has appeared in the literature are approximate relations for P_c^{int}, $\hat{P}_c^{int}$, P_c^{st}, and $\hat{P}_c^{st}$ which depend on certain additional assumptions concerning the magnitudes R_p and R_B that have never been clearly delineated in the literature; these are summarized below.

From [36] and [38] we obtain the so-called limiting 'efficiencies'

$$E_c^{int} = \lim_{R_p \to 0} P_c^{int} \equiv \frac{|G|}{1 + |G|} \qquad [40]$$

and

$$E_c^{st} = \lim_{R_p \to 0} P_c^{st} \equiv \frac{|G|}{1 + |G|} \qquad [41]$$

The result in [41] has appeared in Flint and Howarth (7). The result in [41] also follows from an approximate relation for P_c^{int} which is listed in Table 1 of Nguyen-Van (9).

The most familiar approximate relation in the literature for the probability of collision is the one for Stokes flow, $\hat{P}_c^{st}$, which we indicate below. Actually the oldest form of approximate relation is that for potential flow $\hat{P}_c^{pot}$, $\hat{P}_c^{pot} = 3\left(\frac{R_p}{R_B}\right)$, which was first given by Sutherland (2), where 'pot' denotes potential flow around the bubble and $\hat{}$ indicates that $G \approx 0$, as well as $St \approx 0$.

To initiate the delineation of the various approximate results we assume in [39] that

$$R_p + R_B \simeq R_B \qquad [42]$$

and

$$\left(\frac{R_p}{R_B}\right)^3 << \left(\frac{R_p}{R_B}\right)^2 \qquad [43]$$

In this case, we obtain from [39]

$$\hat{P}_c^{st} \simeq \left(\frac{3}{2}\right)\frac{R_p^2}{R_B^2} \qquad [44]$$

a well-known result that has been often cited, e.g. Schulze (6), but never clearly identified as an approximate relationship; the same degree of approximation as that indicted in both [42] and [43] allows one to conclude, as a consequence of [38], that

$$P_c^{st} \simeq \frac{3}{2(1+|G|)}\left(\frac{R_p^2}{R_B^2}\right) + \frac{|G|}{1+|G|} \qquad [45]$$

The result in [45] appears as the first entry of Table 1 in Nguyen-Van (9) but a derivation of this (albeit) approximate result does not appear in the reference cited there, i.e., in Gaudin (26). Turning to the exact expression for P_c^{int}, i.e., [36] we now assume the validity of both [42] and [43] and, thus, deduce that

$$P_c^{int} \simeq \frac{1}{1+|G|}\left[\left(\frac{3}{2}+4Re_B^*\right)\frac{R_p^2}{R_B^2}\right] + \frac{|G|}{1+|G|} \qquad [46]$$

The (approximate) result in [46] appears as the fourth entry in Table 1 of Nguyen-Van (9) but does not appear in the references cited there, e.g., in Yoon and Luttrell (1); what does appear in (1), albeit without a derivation, is the approximate result for $\hat{P}_c^{int}$ which follows either from [46] by setting $G = 0$, i.e.,

$$\hat{P}_c^{int} = \left(\frac{3}{2}+4Re_B^*\right)\frac{R_p^2}{R_B^2} \qquad [47]$$

or from the exact result [37] by employing the assumptions [42] and [43].

Model Validation

Direct experimental observations of the collision process are very complicated because it is difficult to isolate this microprocess from the other microprocesses in actual flotation separation. However, attempts to experimentally record P_c have been made by a few researchers addressing mineral flotation (1, 3, 8, 9, 14, 15), and these data have been compared to the model presented above.

For these comparisons, considerable effort has been made to match the experimental conditions as closely as possible. Specific parameters of importance are the bubble rise velocity and the particle and fluid thermophysical properties. It was assumed that all experiments were performed in a fluid with properties corresponding to those of water. In all cases, the particular particles used in the experiments were identified by name, but when the density was not provided, a value was chosen based on available tabulated data. The most difficult parameter to match was the bubble rise velocity because this parameter was not always provided for each experimental condition.

Predictions were first compared to experimental data presented by Anfruns and Kitchener (14, 15). They experimentally studied the probability of collision as a single bubble rose through a dilute suspension of quartz particles with a measured size distribution. Five size fractions of quartz were used with mean diameters of 12.0, 18.0, 24.6, 31.4, and 40.5 μm. These particle diameters and a quartz density of 2.65 g/cm^3, obtained from Nguyen-Van and Kmet (8), were used in our predictions. The bubble rise velocity was obtained from data presented in (15) in which experimental results for v_B were presented in terms of bubble diameter.

Figure 2 displays P_c predictions made with [36] incorporating the above experimental

information, and compares the predictions to the experimental data presented by Anfruns and Kitchener (14, 15). In all cases, the P_c calculations overpredict the experimental data. This is probably due to the experiments not sufficiently isolating P_c. In fact, Anfruns and Kitchener actually plot data as "'Efficiency' of Collection (E_c)," which implies that the experimental data may also include adhesion by sliding and stability effects. Since the overall collection efficiency is assumed to be the product of each flotation microprocess efficiency (6), the fact that the P_c predictions over estimate the experimental data is not surprising. This discrepancy was also highlighted by Nguyen-Van and Kmet (8) in which they state: "In our opinion, the experimental results done by these authors [Anfruns and Kitchener] refer rather to [a] collection efficiency than to [a] collision one."

Yoon and Luttrell (1, 3) also present mineral particle flotation data to which P_c model predictions are compared. The experimental set up in these experiments was similar to Anfruns and Kitchener (14, 15); however, they utilized very hydrophobic Buller seam coal particles with 0.13% ash content and mean diameters of 11.4, 31.0, and 40.1 μm in their experiments. According to Yoon and Luttrell (1), the probability of collection they recorded should closely match P_c since the probability of adhesion by sliding for very hydrophobic particles should approach unity. In these comparisons, the particle density was specified to be 1.3 g/cm^3 and the bubble rise velocity was determined from a curve-fit to original bubble rise velocity data of Yoon and Luttrell[1]. Therefore, the bubble rise velocity was calculated from

$$v_B = 10.64(d_B^{1.13}) \qquad [48]$$

where d_B and v_B have units of mm and cm/s, respectively.

[1]Values provided by a reviewer.

Figure 3 compares our P_c predictions to the results of Yoon and Luttrell (1, 3). Their predictions (i.e., [47]) are also included in Fig. 3. Our predictions do very well at predicting P_c, particularly for the smaller particle diameters of 11.4 and 31.0 μm. At $d_p = 40.1\mu m$, [36] underpredicts the data slightly. However, the general trends are followed closely for all particle diameters considered. Our predictions do not differ significantly from the predictions of Yoon and Luttrell because the experimental conditions used to generate Fig. 3 include $R_p << R_B$ and $|G|$ on the order of 0.01 (or less), which satisfy the restrictions on [47].

Nguyen-Van (9) also presented P_c experimental data for two different particle types; quartz ($\rho_p = 2.65\ g/cm^3$, $R_p = 7.75\mu m$) and galena ($\rho_p = 7.5\ g/cm^3$, $R_p = 6.25\mu m$). Property data were obtained from Nguyen-Van and Kmet (8). These experiments involved a fixed bubble held in place on a capillary tube with fluid flowing past the bubble. A dilute particle suspension was injected above the bubble from a second (movable) capillary tube and was entrained in the moving fluid. Particle collisions with the fixed bubble were visually observed. This method allowed for R_c (see Fig. 1) to be experimentally determined. Since the bubble was fixed in these experiments, the bubble rise velocity was equivalent to the fluid velocity flowing past the bubble. The bubble rise velocity was obtained indirectly through Re_B from the following relationship

$$R_B = \left[\frac{9\mu_\ell^2 Re_B(1 + 0.15Re_B^{0.687})}{4\rho_\ell^2 g}\right]^{1/3} \qquad [49]$$

which was presented in (8) and claimed to agree with experimental data.

Figure 4 presents the quartz data from Nguyen-Van (9). Nguyen-Van also developed a prediction for P_c, and this is also shown in the figure. This prediction includes the possibility that the maximum collision angle may be less than 90° from the stagnation point on the

bubble. This prediction has the form

$$P_c = \frac{1}{1+|G|}\left(\frac{R_p}{R_B}\right)^2 \left[\frac{\sqrt{(X+C)^2+3Y^2}-(X+C)}{13.5Y^2}\right]\left[\sqrt{(X+C)^2+3Y^2}+2(X+C)\right]^2 \quad [50]$$

where

$$C = \frac{2R_B^2\Delta\rho g}{9\mu_\ell v_B} \quad [51]$$

$$X = 1.5\left[1+\frac{3Re_B/16}{1+0.309Re_B^{0.694}}\right] \quad [52]$$

$$Y = \frac{3Re_B/8}{1+0.217Re_B^{0.518}} \quad [53]$$

As one can easily see that this P_c prediction is rather complicated, but the Nguyen-Van P_c prediction follows the experimental data very closely. Our P_c prediction [36] has a much simpler form and also does a good job of following the data. The largest discrepancy is at the largest R_B values, but this is still within $\sim 25\%$ of the experimental data. The deviation between our prediction and the experimental data may be due to the collision angle having an effect at these conditions. The inclusion of assumptions [42] and [43] yields [46], which is also shown in Fig. 4. This result does not significantly differ from that of [36] because the experimental conditions satisfy the assumptions incorporated into this approximation. The predictions of Yoon and Luttrell (1) [47] are also shown in Fig. 4 and underpredict the experimental results, indicating that $|G|$ has a significant effect for these experimental conditions.

Figure 5 reveals the same type of comparisons, but for the galena data of Nguyen-Van (9). Galena has a much larger density than that of quartz, so particle settling velocity is much more significant. This is evident by the fact that the Yoon and Luttrell (1) predictions significantly underpredict the experimental data. Our current P_c predictions [36] and [46] (with the associated assumptions) do a very good job of predicting the experimentally

determined P_c values. The more complicated P_c prediction of Nguyen-Van (9) also does a very good job.

In summary, our model for the probability of collision does a very good job of predicting available experimental results for P_c. The model is less complicated than that proposed by Nguyen-Van (9), but just as accurate, and is much improved over the model of Yoon and Luttrell (1).

Parametric Variations

The exact intermediate flow solution for P_c [36] can be rearranged to show that three dimensionless groups of R_p/R_B, Re_B, and $|G|$ are the only parameters that influence the probability of collision. If $|G| \approx 0$, the particle settling velocity does not affect P_c. This result, and the approximate result of Yoon and Luttrell (1) [47], are shown in Fig. 6 for $Re_B \leq 500$. When $Re_B = 0$, Stokes flow conditions prevail (i.e., [39]), and a minimum P_c results for all $R_p/R_B < 1$, with P_c increasing as R_p/R_B increases. Increasing Re_B for a fixed R_p/R_B increases P_c and these values run parallel to those predicted by Stokes flow. The applicability of these results at $Re_B = 500$ is questionable because the stream function for intermediate flow was developed for $0 \leq Re_B \leq 100$ (1); however, Yoon and Luttrell (1) state that it "may be applicable for $Re_B > 100$, although no experimental (streamline) date [were] available in the present work." In Fig. 6, unrealistic predictions from [36] ($P_c > 1$) result when $R_p/R_B \gtrsim 0.3$ and $Re_B = 500$. This result will be further discussed below. The exact and approximate solutions follow closely to one another for small values of R_p/R_B, and at $R_p/R_B = 0.1$, the approximate solution presented by Yoon and Luttrell (1) over predicts P_c by approximately 25% when $Re_B = 0$ and by more than 35% when $Re_B = 500$. As expected, increasing R_p/R_B further toward 1 increases this difference because the approximations of

Yoon and Luttrell (i.e., [42] and [43] with $|G| = 0$) are no longer valid. Applying these approximations when $R_p/R_B \rightarrow 1$ results in [47] predicting $P_c > 1$ for all Re_B.

Figure 7 reveals the exact predictions for P_c [36] for $0 \leq Re_B \leq 500$ and $|G| = 0.1$. The exact prediction for Stokes flow [38] corresponds to $Re_B = 0$. The bubble Reynolds number has a negligible effect on P_c when $R_p/R_B \lesssim 0.03$, and a constant P_c results, which is a function of $|G|$ (as shown in Fig. 8). When $R_p/R_B \gtrsim 0.03$, P_c increases exponentially with increasing R_p/R_B. Additionally, the increase in P_c is more abrupt as Re_B increases. When $R_p/R_B = 1$, $P_c \leq 1$ for $Re_B \leq 100$. As previously stated, these predictions are questionable when $Re_B > 100$ because the stream function used to generate [36] includes data only up to $Re_B = 100$ (1). In our predictions, when $Re_B = 500$ and $R_p/R_B \gtrsim 0.3$, $P_c > 1$, but P_c is independent of Re_B when $R_p/R_B \lesssim 0.03$ and [36] can be used outside its given Re_B range under these specific conditions.

Similar calculations to those presented above have been completed using [36] for fixed Re_B over the given R_p/R_B range and for selected values of $|G|$. Figure 8 reveals one such plot for $Re_B = 10$. The approximate solution [46], which incorporates assumptions [42] and [43], is also shown in Fig. 8. When $|G| = 0$, the approximate solution corresponds to the predictions of Yoon and Luttrell (1). When R_p/R_B is small, P_c increases with increasing $|G|$ by several orders of magnitude when compared to the $|G| = 0$ predictions, implying the particle settling velocity significantly enhances the collision probability when collision occurs between a particle that is much smaller than the colliding bubble. This would be particularly true for particles with a density much larger than that of water. The increase in P_c with increasing $|G|$ is much smaller when a particle and bubble size are the same order of magnitude (with $R_p < R_B$), and as $R_p/R_B \rightarrow 1$, P_c predictions approach the same value independent of $|G|$. In Fig. 8, all P_c predictions are less than 1 for $R_p/R_B \leq 1$,

except the approximate solution [46] when $R_p/R_B \rightarrow 1$ because the assumptions [42] and [43] are no longer valid. The approximate P_c predictions [46] and the exact P_c predictions [36] are equivalent for small R_p/R_B. When $R_p/R_B \approx 0.03,\ 0.05$, and 0.2, the approximate solution begins to deviate from the exact solution when $|G| = 0,\ 0.01$, and 1, respectively, and $Re_B = 10$. Also, as R_p/R_B increases, the approximate solution asymptotes to the Yoon and Luttrell (1) solution [47], which does not include the effects of particle settling velocity. This figure reveals that particle settling velocity is important at small values of R_p/R_B and assumptions [42] and [43] are not. Conversely, as $R_p/R_B \rightarrow 1$, assumptions [42] and [43] dominate and the inclusion of $|G|$ has only a secondary effect.

Additional calculations have been performed for fixed values of R_p/R_B while both $|G|$ and Re_B are varied. These predictions result in contour plots of P_c for each fixed value of R_p/R_B. When $R_p/R_B = 0.1$ (Fig. 9), the contour lines are plotted with logarithmic increments, showing that P_c varies by almost two orders of magnitude for the given conditions. For $R_p/R_B = 0.1$, P_c is a strong function of $|G|$ for all values of Re_B. In contrast, P_c is a function of Re_B when $|G| < 0.2$ and is independent of Re_B when $|G| \gtrsim 0.2$.

At $R_p/R_B = 0.9$ (Fig. 10), P_c contours are now plotted on a linear scale with major divisions (solid lines) corresponding to P_c values in increments of 0.1 and minor divisions (dashed lines) representing P_c values in increments of 0.05. Under these conditions, P_c is independent of Re_B only for small Re_B and large $|G|$. Conversely, P_c is independent of $|G|$ when $|G|$ is small and Re_B is large. Therefore, as discussed earlier, when R_p/R_B is large, particle settling velocity only plays a minor role and only when Re_B is small and $|G|$ is large.

Summary

An exact solution for the probability of collision, P_c, has been developed based on the

intermediate flow field of Yoon and Luttrell (1). This solution is a function of three dimensionless parameters including the magnitude of the dimensionless particle settling velocity, $|G|$, the bubble Reynolds number, Re_B, and the ratio of particle to bubble radius, R_p/R_B. The resulting expression [36] only assumes that the bubble and particle are spherical and that $R_p < R_B$ (the restriction that $R_p << R_B$ is *not* required).

The new prediction for P_c presented here does a good job of predicting available experimental data. The inclusion of the particle settling velocity is very important, particularly when the particles have a density much higher than that of water. Additionally, the form of P_c derived here is much simpler than that proposed by Nguyen-Van (9), and just as accurate at predicting experimental results.

Selected P_c predictions have also been presented using [36] for $0 \leq Re_B \leq 500$, $0 \leq |G| \leq 1$, and $0.001 \leq R_p/R_B < 1$. In general, P_c is independent of Re_B when $R_p/R_B \lesssim 0.03$, the particle settling velocity is important for small values of R_p/R_B, and R_p/R_B dominates as $R_p/R_B \rightarrow 1$.

ACKNOWLEDGMENT

The work described in this paper was funded by the Member Companies of the Institute of Paper Science and Technology. Their continued support is gratefully acknowledged.

REFERENCES

1. Yoon, R.H., and Luttrell, G.H., *Miner. Process. Extract. Metal. Rev.* **5**, 101 (1989).
2. Sutherland, K.L., *J. Phys. Chem.* **52**, 394 (1948).
3. Luttrell, G.H., and Yoon, R.H., *J. Colloid Interface Sci.* **154**, 129 (1992).
4. Ahmed, N., and Jameson, G.J., *Miner. Process. Extract. Metal. Rev.* **5**, 77 (1989).
5. Schulze, H.J., *in* "Coagulation and Flocculation" (B. Dobias, Ed.), p. 321. Marcel Dekker, New York, 1993.
6. Schulze, H.J., "Physicochemical Elementary Processes in Flotation." Elsevier, Amsterdam, 1984.
7. Flint, L.R., and Howarth, W.J., *Chem. Eng. Sci.* **26**, 1155 (1971).
8. Nguyen-Van, A., and Kmet, S., *Int. J. Mineral Processing* **35**, 205 (1992).
9. Nguyen-Van, A., *J. Colloid Interface Sci.* **162**, 123 (1994).
10. Weber, M.E., *J. Separ. Proc. Technol.* **2**, 29 (1981).
11. Weber, M.E., and Paddock, *J. Colloid Interface Sci.* **94**, 328 (1983).
12. Reay, D., and Ratcliff, G.A., *The Canad. J. Chem. Eng.* **51**, 178 (1973).
13. Dobby, G.S., and Finch, J.A., *Int. J. Min. Process* **21**, 241 (1987).
14. Anfruns, J.P., and Kitchener, J.A., *Trans. Inst. Min. Metall., Sect. C.* **86**, C9 (1977).
15. Anfruns, J.P., and Kitchener, J.A., *in* "Flotation," (M. Fuerstenau, Ed.), p. 625. AIME, New York, 1976.
16. Spielman, L.A., *Ann. Rev. Fluid Mech.* **9**, 297 (1977).
17. Michael, D.H., and Norey, P.W., *J. Fluid Mech.* **37**. 565 (1969).
18. Bloom, F., and Heindel, T.J., *Mathl. Comput. Modelling* **25**, 13 (1997).
19. Heindel, T.J., and Bloom, F., *in* "1997 TAPPI Recycling Symposium Proceedings," p. 101. TAPPI Press, Atlanta, 1997.
20. Bloom, F., and Heindel, T.J., *J. Colloid Interface Sci.* **190**, 182 (1997).
21. Matis, K.A., and Zouboulis, A.I., *in* "Flotation Science and Engineering," (K.A. Matis, Ed.), p. 63. Marcel Dekker, New York, 1995.

22. Clift, R., Grace, J.R., and Weber, M.E., "Bubbles, Drops, and Particles," Academic Press, New York, 1978.

23. Cheremisinoff, M.P., *in* "Encyclopedia of Fluid Mechanics, *5: Slurry Flow Technology,*" (N.P. Cheremisinoff, Ed.), p. 685. Gulf Publishing Company, London, 1986.

24. Seeley, L.E., Hummel, R.L., and Smith, J.W., *J. Fluid Mech.* **68**, 591 (1975).

25. Batchelor, G.K., "An Introduction to Fluid Dynamics," Cambridge Univ. Press, Cambridge, U.K., 1990.

26. Gaudin, A.M., "Flotation," 2nd ed., McGraw-Hill, New York, 1957.

Figure Captions

Figure 1: Particle colliding with a bubble at $\theta_c = \pi/2$.

Figure 2: Experimental data for P_c obtained by Anfruns and Kitchener (14, 15) and the associated numerical predictions from the P_c model [36].

Figure 3: Comparison between the experimental P_c data obtained from Yoon and Luttrell (1) and numerical predictions for P_c.

Figure 4: Comparison between experimental data obtained from Nguyen-Van (9) for quartz particles and numerical predictions for P_c.

Figure 5: Comparison between experimental data obtained from Nguyen-Van (9) for galena particles and numerical predictions for P_c.

Figure 6: Exact and approximate P_c predictions with $0 \leq Re_B \leq 500$ and $|G| = 0$.

Figure 7: Exact P_c predictions for $0 \leq Re_B \leq 500$ and $|G| = 0.1$.

Figure 8: Exact and approximate P_c predictions for $|G| = 0,\ 0.01$, and 1 and $Re_B = 10$.

Figure 9: Contours of P_c when $R_p/R_B = 0.1$. Note the P_c scale is logarithmic.

Figure 10: Contours of P_c when $R_p/R_B = 0.9$. Note the P_c scale is linear.

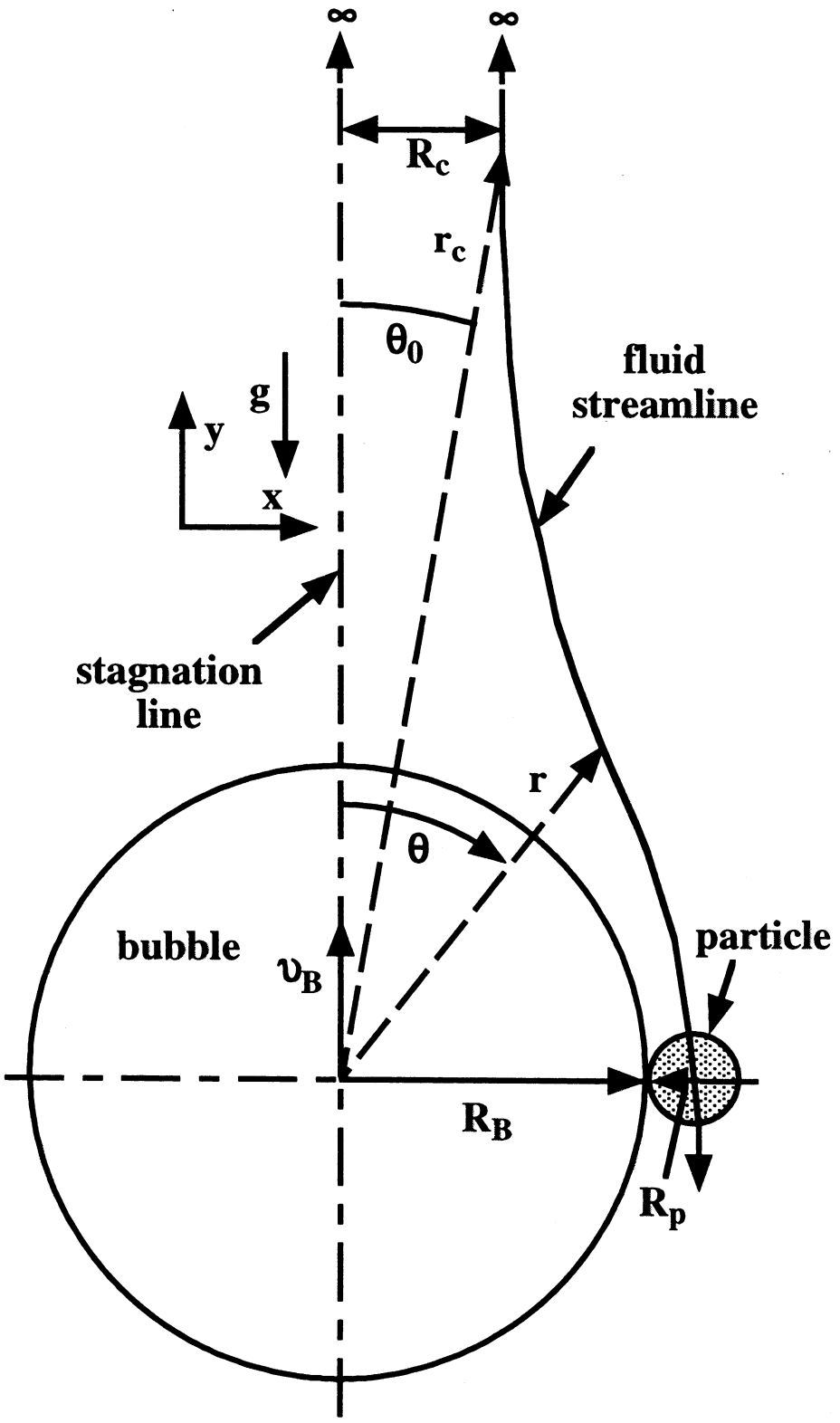
∞
∞
R_c
r_c
θ_0
fluid
streamline
g
y
x
stagnation
line
r
θ
bubble
υ_B
particle
R_B
R_p

Figure 1

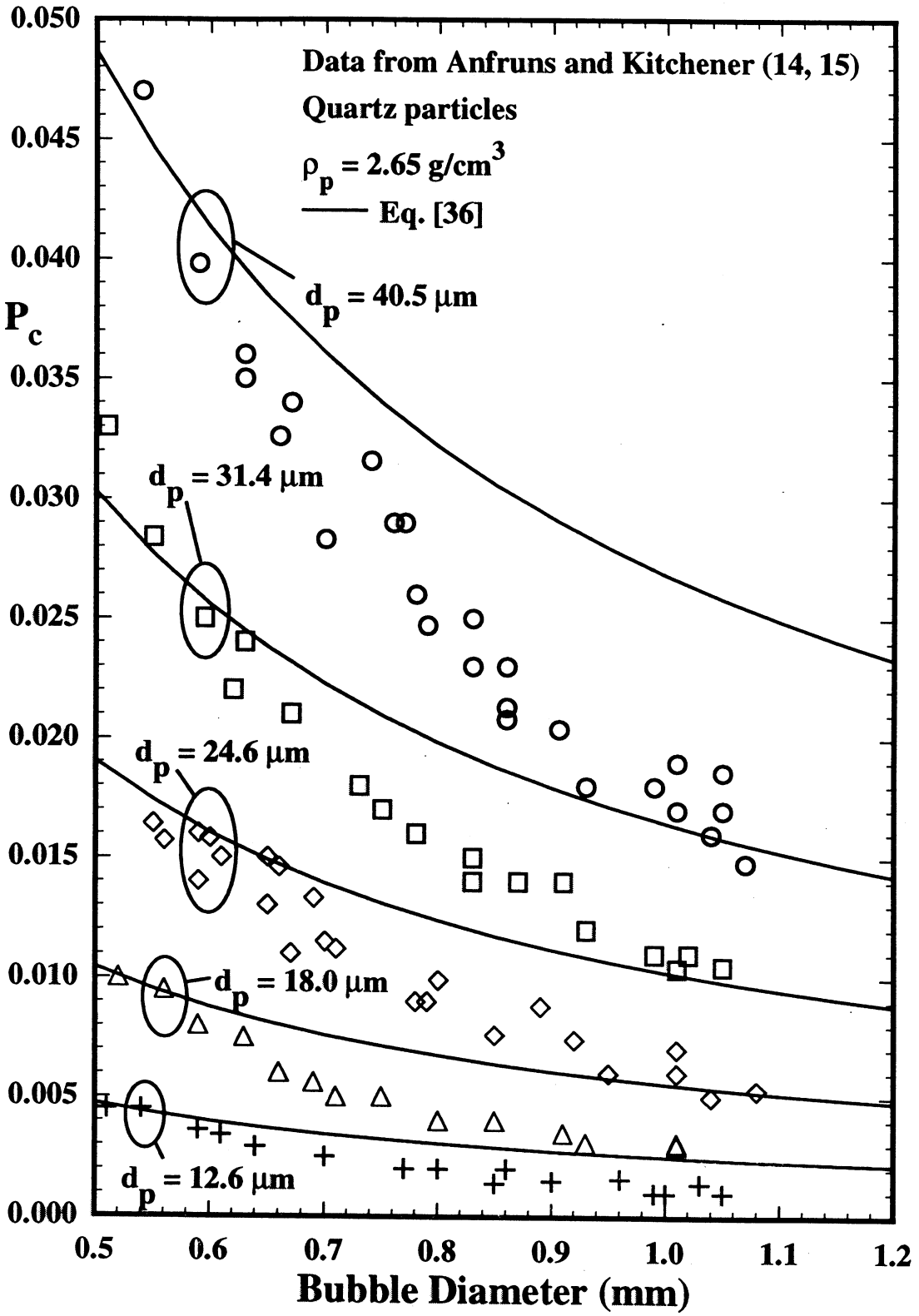
Data from Anfruns and Kitchener (14, 15)
Quartz particles
ρ_p = 2.65 g/cm^3
Eq. [36]
d_p = 40.5 μm
d_p = 31.4 μm
d_p = 24.6 μm
d_p = 18.0 μm
d_p = 12.6 μm
P_c
0.050
0.045
0.040
0.035
0.030
0.025
0.020
0.015
0.010
0.005
0.000
0.5
0.6
0.7
0.8
0.9
1.0
1.1
1.2
Bubble Diameter (mm)

Figure 2

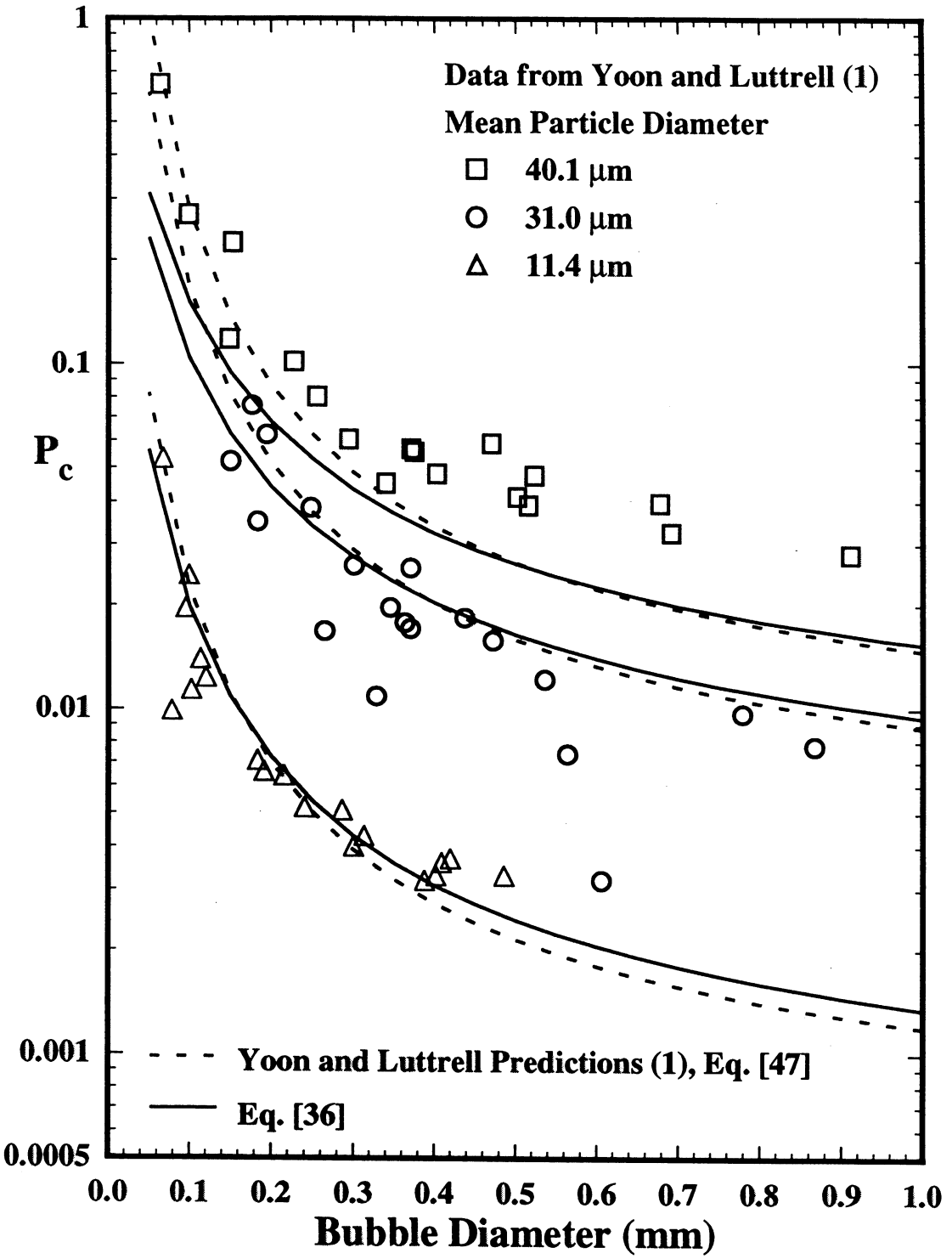
1
0.1
0.01
0.001
0.0005
P_c
Data from Yoon and Luttrell (1)
Mean Particle Diameter
40.1 μm
31.0 μm
11.4 μm
Yoon and Luttrell Predictions (1), Eq. [47]
Eq. [36]
0.0
0.1
0.2
0.3
0.4
0.5
0.6
0.7
0.8
0.9
1.0
Bubble Diameter (mm)

Figure 3

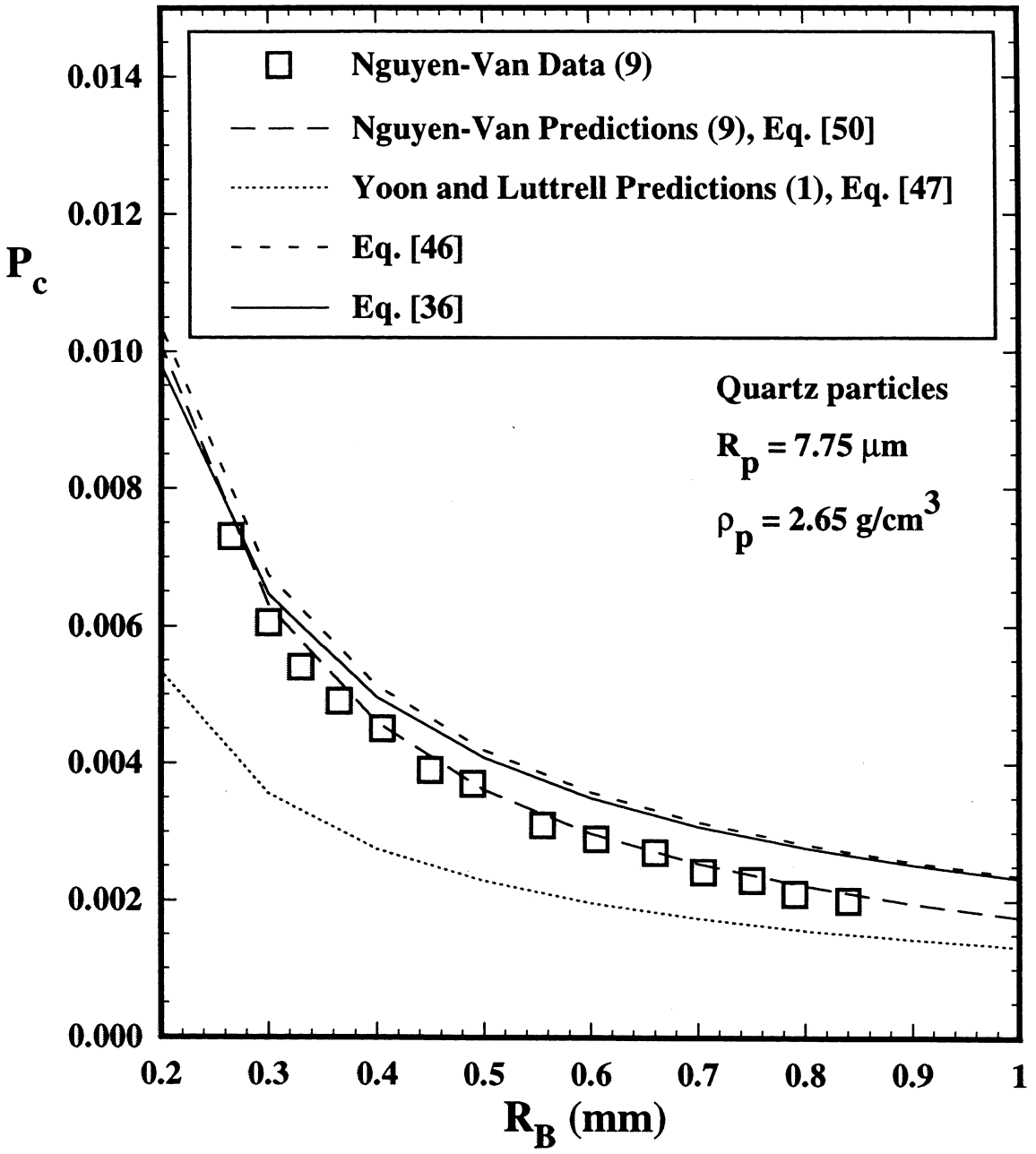
Nguyen-Van Data (9)
Nguyen-Van Predictions (9), Eq. [50]
Yoon and Luttrell Predictions (1), Eq. [47]
Eq. [46]
Eq. [36]
Quartz particles
R_p = 7.75 μm
ρ_p = 2.65 g/cm^3
P_c
0.014
0.012
0.010
0.008
0.006
0.004
0.002
0.000
0.2
0.3
0.4
0.5
0.6
0.7
0.8
0.9
1
R_B (mm)

Figure 4

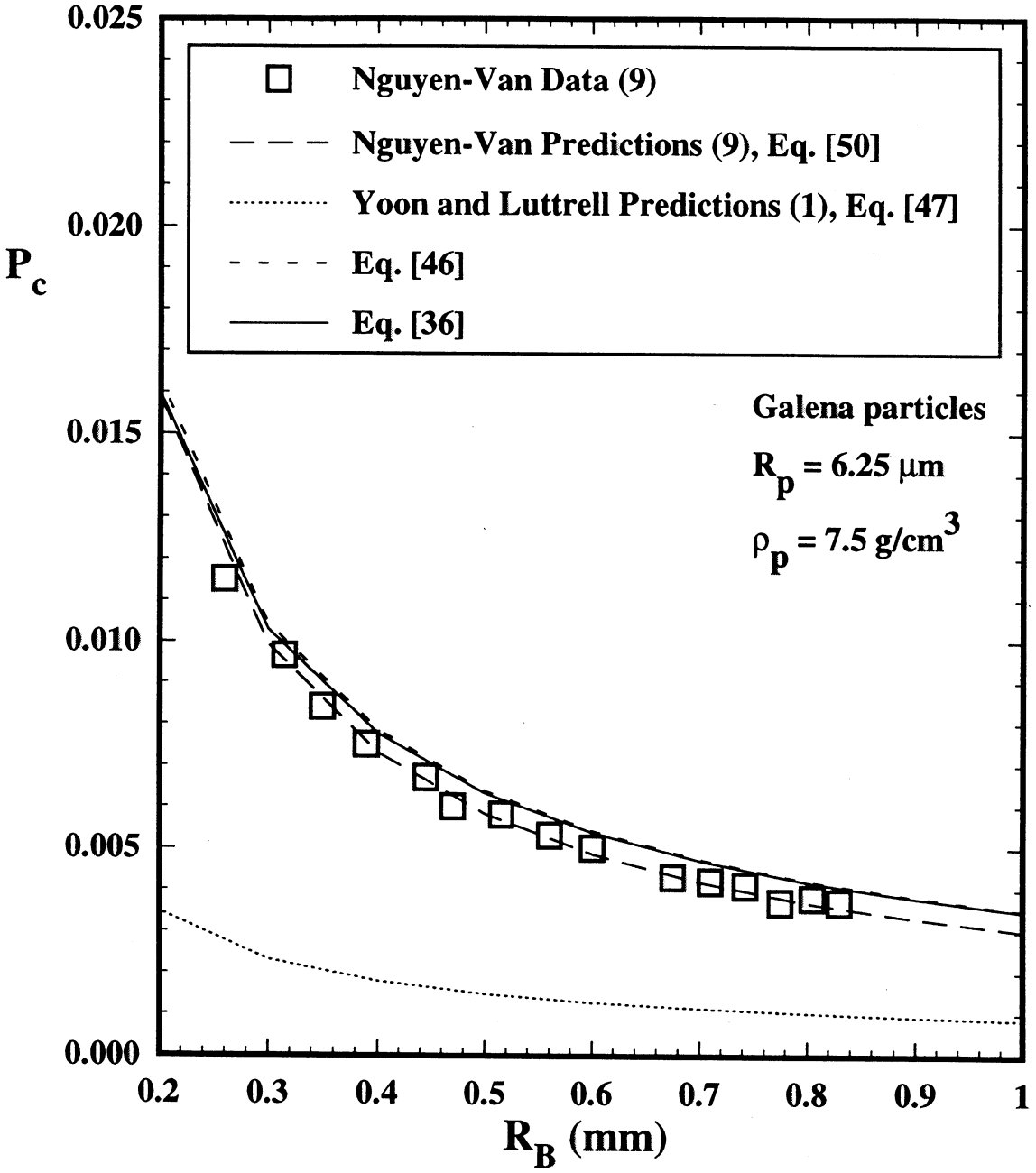
0.025
0.020
0.015
0.010
0.005
0.000
P_c
Nguyen-Van Data (9)
Nguyen-Van Predictions (9), Eq. [50]
Yoon and Luttrell Predictions (1), Eq. [47]
Eq. [46]
Eq. [36]
Galena particles
R_p = 6.25 μm
ρ_p = 7.5 g/cm^3
0.2
0.3
0.4
0.5
0.6
0.7
0.8
0.9
1
R_B (mm)

Figure 5

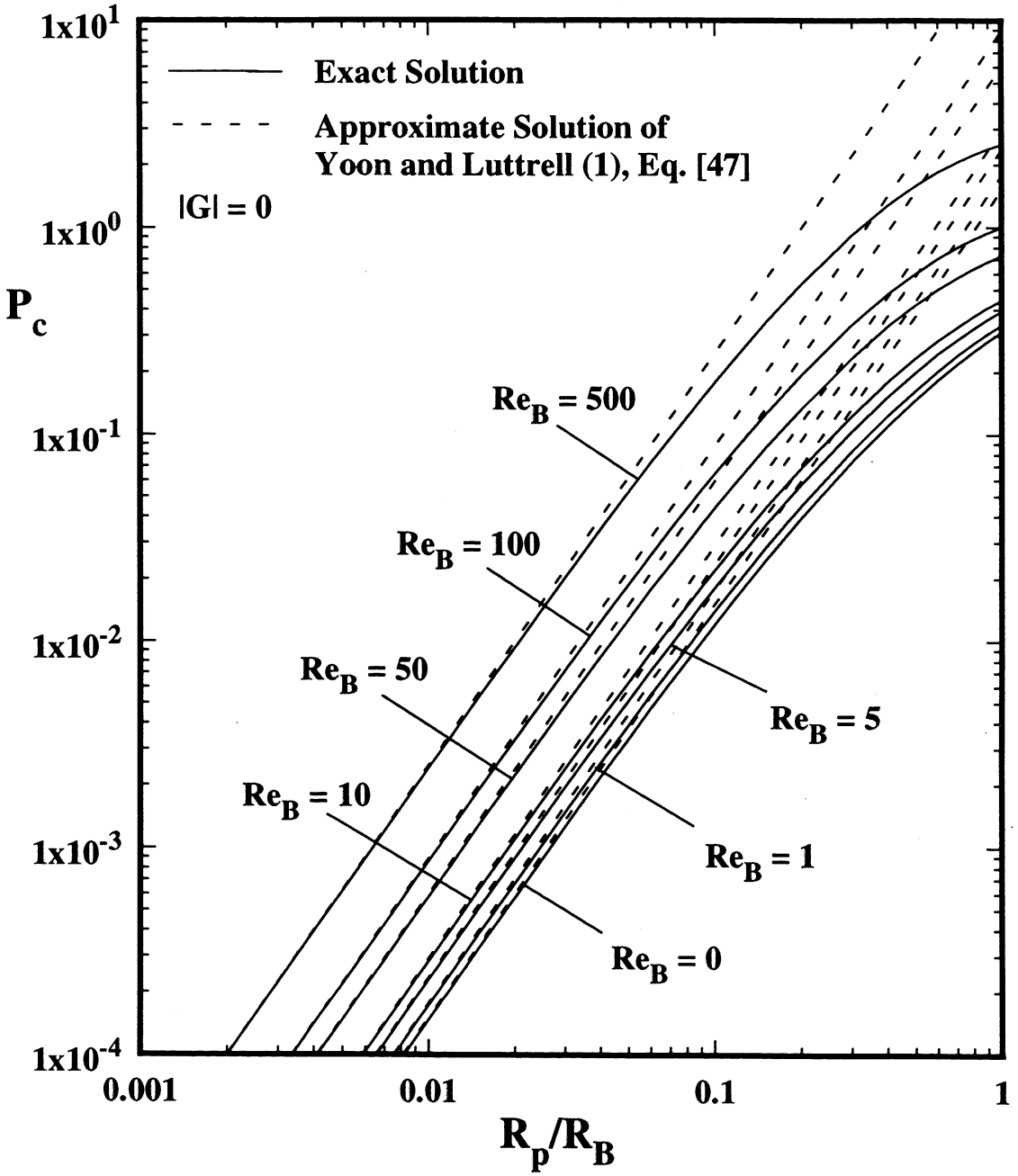
Exact Solution
Approximate Solution of
Yoon and Luttrell (1), Eq. [47]
|G| = 0
Re_B = 500
Re_B = 100
Re_B = 50
Re_B = 10
Re_B = 5
Re_B = 1
Re_B = 0
P_c
R_p/R_B
1x10^1
1x10^0
1x10^-1
1x10^-2
1x10^-3
1x10^-4
0.001
0.01
0.1
1

Figure 6

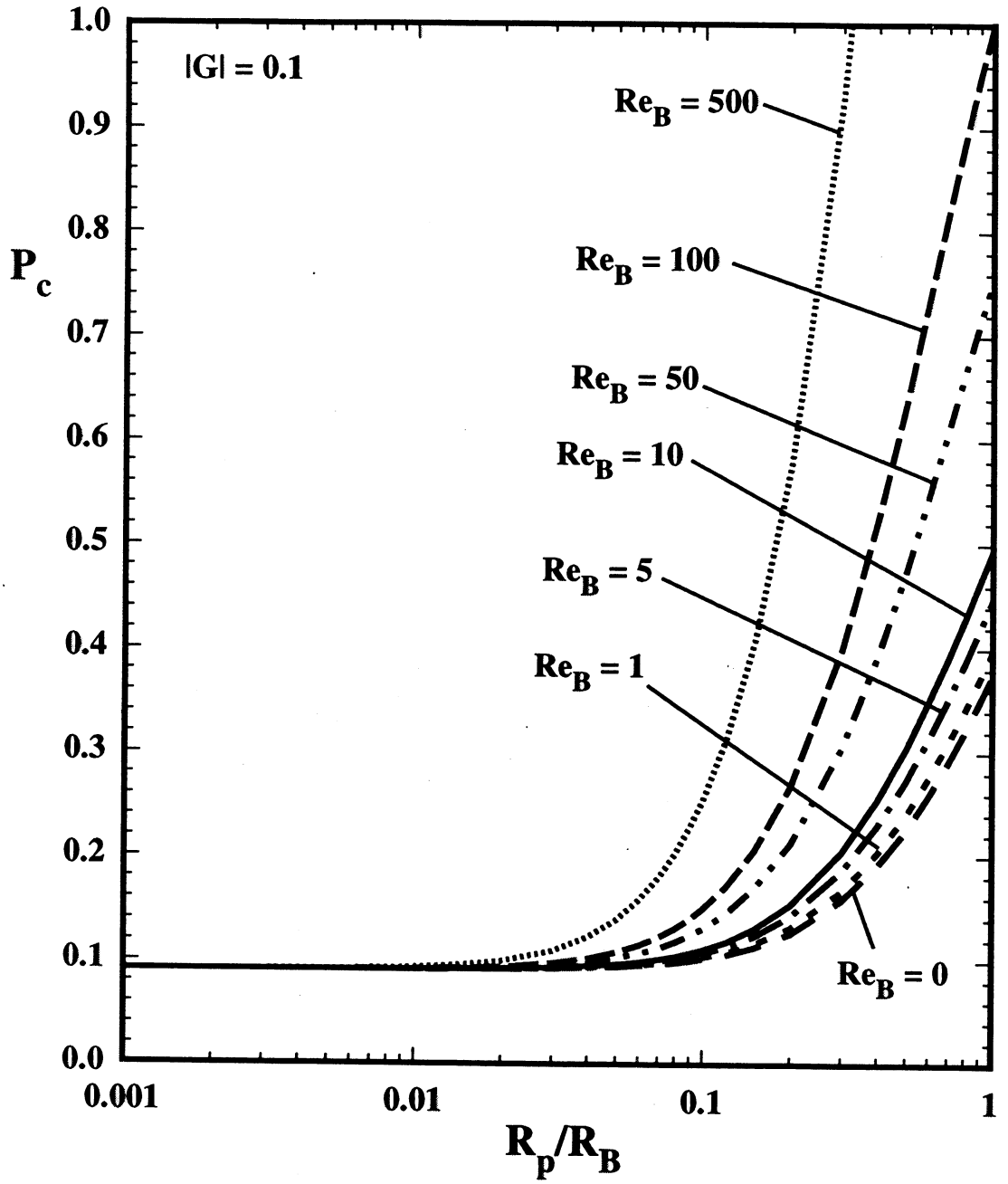
|G| = 0.1
Re_B = 500
Re_B = 100
Re_B = 50
Re_B = 10
Re_B = 5
Re_B = 1
Re_B = 0
P_c
R_p/R_B
1.0
0.9
0.8
0.7
0.6
0.5
0.4
0.3
0.2
0.1
0.0
0.001
0.01
0.1
1

Figure 7

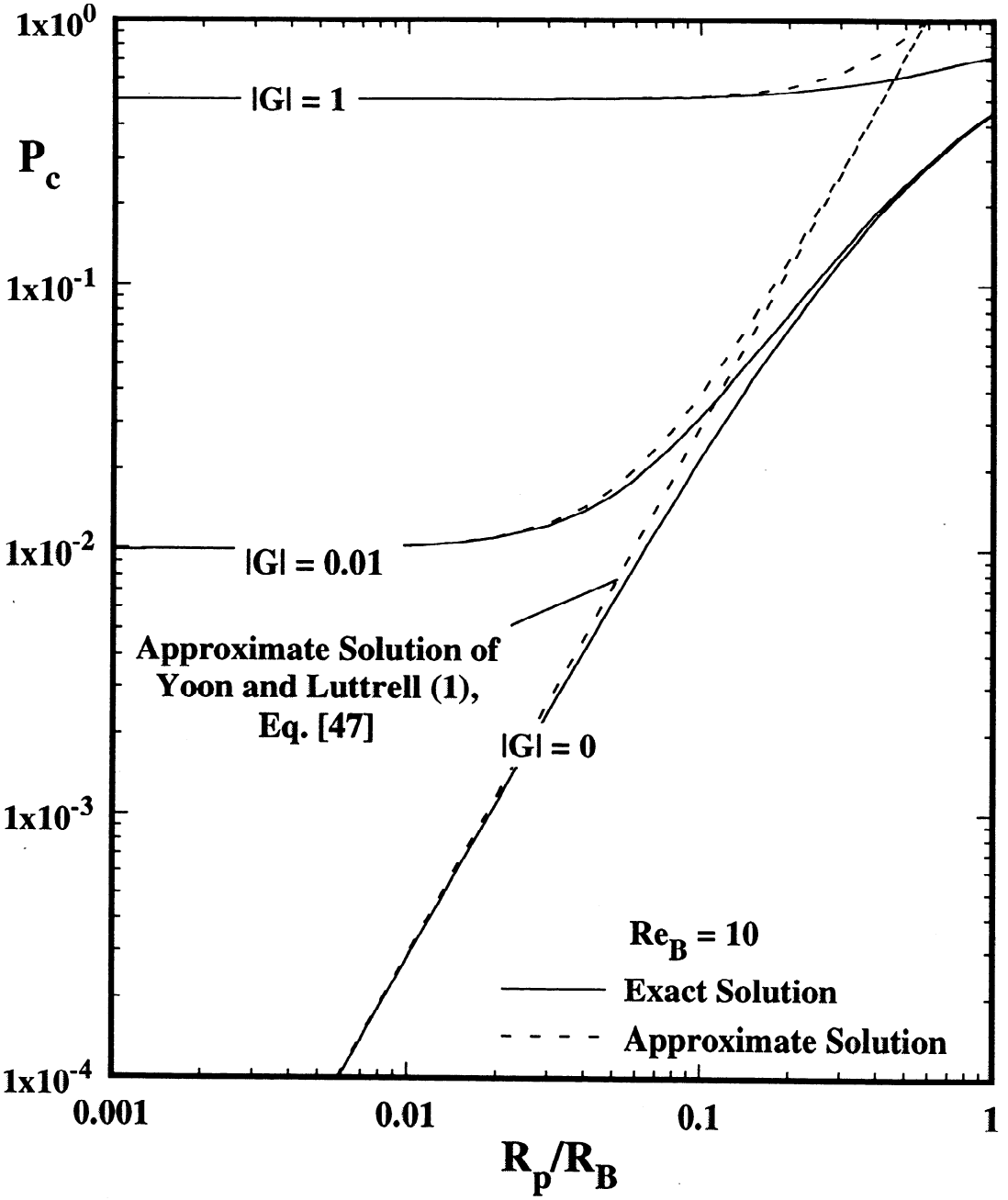
1x10^0
1x10^-1
1x10^-2
1x10^-3
1x10^-4
P_c
|G| = 1
|G| = 0.01
|G| = 0
Approximate Solution of
Yoon and Luttrell (1),
Eq. [47]
Re_B = 10
Exact Solution
Approximate Solution
0.001
0.01
0.1
1
R_p/R_B

Figure 8

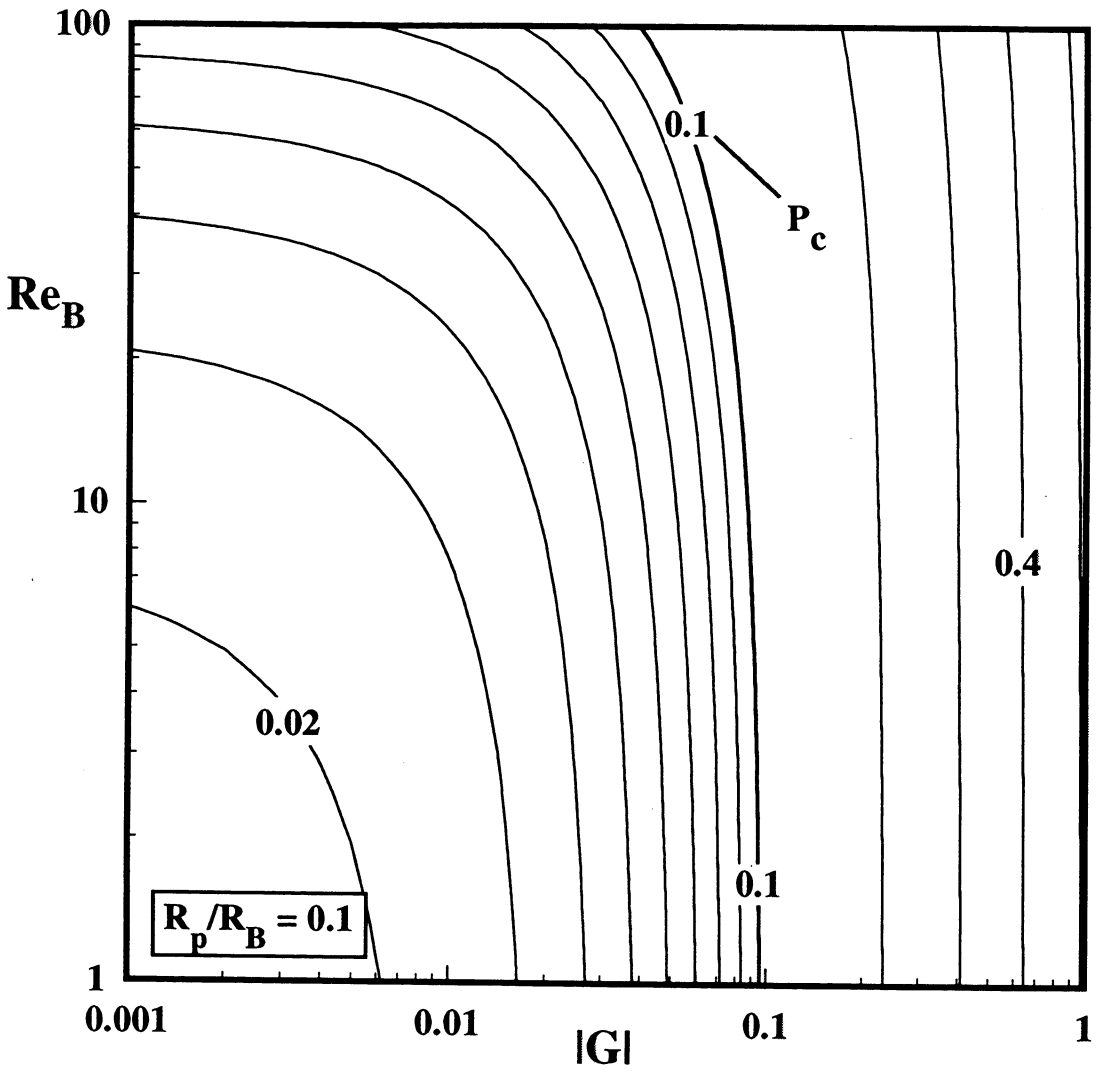

Figure 9

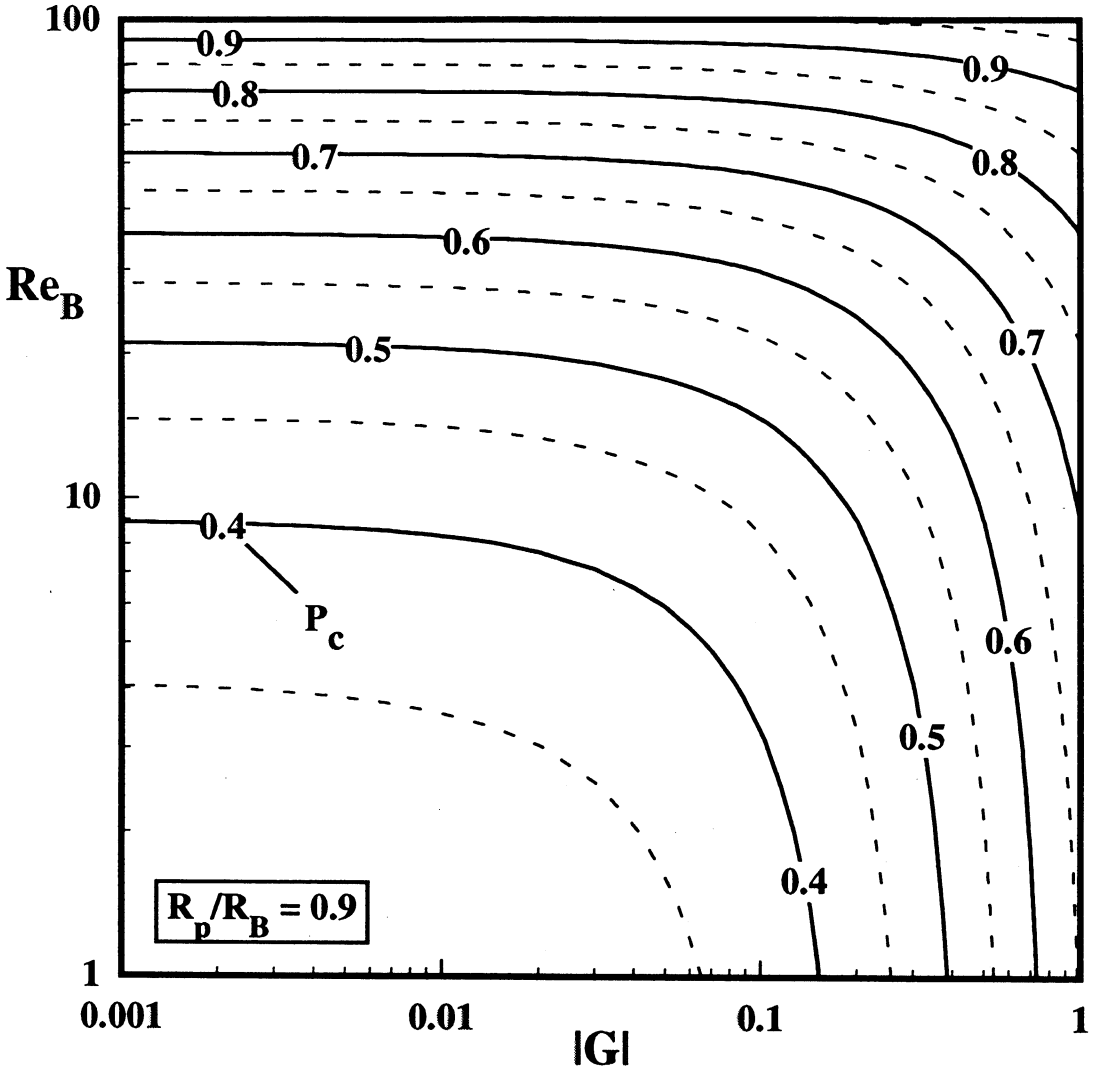

Figure 10